

Structure of Thermosensitive Poly(*N*-vinylcaprolactam-co-*N*-vinylpyrrolidone) Microgels

Volodymyr Boyko,[†] Sven Richter,^{*,†} Isabelle Grillo,[‡] and Erik Geissler[§]

Institute of Physical Chemistry and Electrochemistry, Dresden University of Technology, Mommsenstrasse 13, D-01062 Dresden, Germany; Institut Laue Langevin, 6 rue Jules Horowitz, B. P. 156, 38042 Grenoble, Cedex 9, France; and Laboratoire de Spectrométrie Physique, CNRS UMR 5588, Université Joseph Fourier de Grenoble, B. P. 87, 38402 St. Martin d'Hères, Cedex, France

Received March 15, 2005

ABSTRACT: The internal structure of thermoreversible poly(*N*-vinylcaprolactam-co-*N*-vinylpyrrolidone) microgels has been studied by static and dynamic light scattering (SLS/DLS) and small-angle neutron scattering (SANS). A dramatic decrease in the radius of gyration R_g and the hydrodynamic radius R_h is observed during the phase transition near 30 °C. At 15 and 30 °C the experimental SLS/SANS curves can be fitted to a model of polydisperse spheres with rough surfaces. The resulting fit parameters are discussed in the framework of changes in the internal structure of the particles during the phase transition. In the completely collapsed state at 50 °C, the scattering response can be described by a modified Porod behavior.

1. Introduction

Aqueous colloidal microgels are an interesting subset of polymer colloids. Microgels have properties in common with water-soluble polymers, water-swollen macrogels, and water-insoluble latex particles. Like macroscopic aqueous gels, colloidal microgels resemble a three-dimensional, covalently cross-linked network. The network is characterized by the degree of swelling, the average cross-link density, and the characteristic time constants for swelling and shrinking, which depend on solvent quality. It is well-known from DLS and SANS studies that several types of heterogeneities occur in macroscopic gels. The difference in reactivity of monomers and cross-linker and complex kinetics lead to the formation of pendant polymer chains, trapped entanglements, and elastically ineffective chains and local clusters with a high cross-linking density. As a result of heterogeneity of a gel, the scattered intensity observed in DLS and SANS can be divided into a static part, which is a result of frozen-in inhomogeneities, and a dynamic part caused by the thermal fluctuations of the network. The structure of macroscopic gels as a function of the method and conditions of preparation has been the topic of intensive studies in the past decade.^{1–5} However, only a few investigations were published on the structure of colloidal microgels. Wu et al.⁶ have studied the kinetic of formation of the microgel based on NIPAm by DLS. They observed much faster consumption of cross-linker than of monomer and, as result, differences in cross-linking density throughout the particle. Kratz et al.^{7,8} found from SANS measurements that the correlation length of NIPAm microgels decreases with increasing cross-linking density and is comparable to that found in macroscopic PNIPAm gels. Saunders proposed a fairly uniform structure within the swollen particles and a core–shell morphology with a relatively thin shell.^{9,10} Fernando-Barbero et al.¹¹ sug-

gested a core–shell structure having different correlation lengths for core and shell, which can be calculated in different q -regimes of SANS.

Scattering methods yield information not only on internal structure (at large scattering vectors q) but also on the form of the particles (low and intermediate q). Microgel particles can be considered as soft deformable colloids. By changing the preparation conditions and the composition of the reaction medium, the interaction potential between microgel particles can vary from star-polymer-like to hard-sphere-like for short-range repulsion. Owing to the complex structure, the scattering intensity from microgels cannot be described by the form factor of homogeneous hard spheres. Burchard et al.¹² used a regularly branched model to describe PVAc microgels in methanol. Kunz et al.¹³ used the radial density distribution to calculate the form factor of PMMA microgels. Varga et al.¹⁴ used a similar approach for PNIPAm microgels, but no universal model was found. Stieger et al. used the form factor of a sphere with an interface that gradually decreases at the surface, developed by Pederson and Svaneborg^{15,16} for block copolymer micelles. Good agreement was observed with this model for PNIPAm microgels measured by SANS¹⁷ and SLS.¹⁸

Here we present a study of microgels based on *N*-vinylcaprolactam (VCL) and *N*-vinylpyrrolidone (VP) by DLS, SLS, and SANS over wide range of scattering vector q . PVCL is a polymer with a lower critical solution temperature (LCST) around 32 °C.¹⁹ Its biocompatibility is potentially favorable for biomedical application materials.²⁰ Because of the difficulties of preparation, only a few reports on the synthesis and characterization of microgels based on PVCL have been published.^{21–23}

2. Experimental Section

2.1. Sample Preparation. The poly(*N*-vinylcaprolactam-co-*N*-vinylpyrrolidone), PVCL/PVP (see Figure 1), microgels were prepared by precipitation copolymerization of *N*-vinylcaprolactam and *N*-vinylpyrrolidone in the presence of cross-linker. Monomers (Aldrich) were distilled under reduced

[†] Dresden University of Technology.

[‡] Institut Laue Langevin.

[§] Université Joseph Fourier de Grenoble.

* Corresponding author: e-mail Sven.Richter@chemie.tu-dresden.de; Ph +49-351-463-32492; Fax +49-351-463-37122.

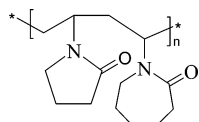


Figure 1. Chemical structure of the repeating unit of PVCL-PVP.

pressure before use. *N,N'*-methylenebis(acrylamide) (MBA, Aldrich) was taken as the cross-linker and was used as received. The initiator was 2,2'-azobis(2-methylpropionamide) dihydrochloride (AMPA, Aldrich), which was also used without further purification. 0.835 g of VCL, 0.19 g of VP, and 0.066 g MBA were dissolved in 95 mL of deuterated water. A double-walled glass reactor equipped with stirrer was purged with nitrogen. The solution of the monomers was placed in the reactor and stirred for 1 h at 70 °C with nitrogen purging. 5 mL of D₂O solution of AMPA (5 g/L) was then added under continuous stirring to initiate the reaction. Duration of the reaction was 8 h.

2.2. Experimental Details. **2.2.1. SANS.** SANS experiments were performed on the D11 instrument at the Institut Laue-Langevin (ILL), Grenoble, with neutron wavelength $\lambda = 13$ Å and wavelength spread $\Delta\lambda/\lambda = 10\%$. The two-dimensional multidetector data were regrouped azimuthally and corrected for solvent background and empty cell scattering. All measurements were carried out with D₂O as the solvent, the samples being placed in quartz cells of thickness 2 mm. Three sample-detector distances were used, 1.6, 6.5, and 28 m. The incoherent scattering of H₂O was used for absolute calibration, following standard procedures and software available at the ILL. The concentration of the microgel sample was 2.5 g/L, and the samples were thermostated to within ± 0.5 °C for each measured temperature.

2.2.2. SLS. To determine the radius of gyration R_g , SLS measurements were made on suspensions in the concentration range 0.01–0.15 g/L, using a modified FICA 50 SLS apparatus (SLS-Systemtechnik G. Baur, Denzlingen, Germany) with a He-Ne laser working at a wavelength of $\lambda = 632.8$ nm. The measuring temperatures were from 15 to 50 °C, and the scattering angle was varied between 15° and 145° in 5° steps. Dispersions were filtered through 5 μ m nylon filters. Typically, the measuring cells were 25 mm quartz tubes, immersed in a dibutyl phthalate bath thermostated within an accuracy of ± 0.1 °C.

The refractive index increment (dn/dc), measured with a DR 1 differential refractometer (SLS-Systemtechnik) at $\lambda = 632.8$ nm, was found to be 0.2229 cm³/g.

2.2.3. DLS. A commercial laser light scattering (LLS) spectrometer (ALV/DLS/SLS-5000) equipped with an ALV-5000/EPP multiple digital time correlator and laser goniometer system ALV/CGS-8F S/N 025 was used with a helium-neon laser (Uniphase 1145P, output power 22 mW, wavelength $\lambda = 632.8$ nm) as the light source. The DLS experiments were carried out as a function of temperature in the range of scattering angles $\theta = 30^\circ$ – 100° . The concentration of the dispersions, which had been previously filtered through 5 μ m nylon filters, was in the range 0.01–0.15 g/L. The samples were held in 10 mm test tubes immersed in a toluene bath whose temperature was controlled to within ± 0.1 °C.

3. Results and Discussion

Combination of VCL with VP leads to the formation of stable microgel dispersions without addition of stabilizer. Because of its hydrophilic nature, PVP units can sterically stabilize microgel particles due to immobilization of PVP on the surface and an increase in the repulsive forces. On the other hand, at the polymerization temperature, VP in the polymer network tends to increase the water solubility of the copolymer. Increased solubility means an increased critical length for oligomer phase separation to form precursor particles and yields larger particles.²⁴

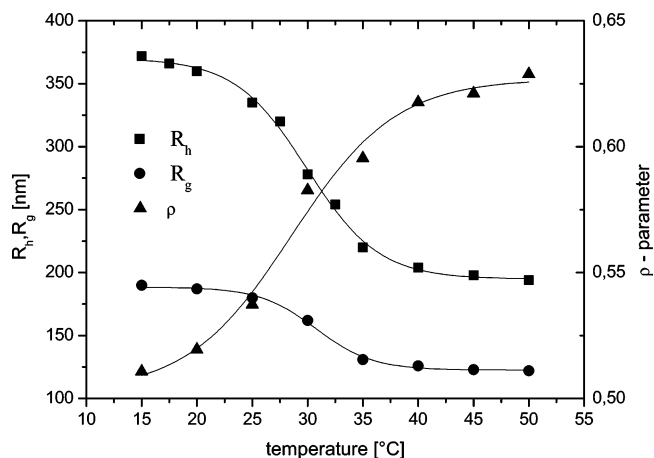


Figure 2. Temperature dependence of the radius of gyration R_g and hydrodynamic radius R_h of the microgels (left-hand scale). Right-hand scale: $\rho = R_g/R_h$.

The influence of the temperature on the size of the microgel particles was investigated by the combined DLS/SLS technique. A continuous decrease of the hydrodynamic radius and the radius of gyration in the range 20–40 °C was observed with an inflection point around 30 °C. As is well-known, the ratio $\rho = R_g/R_h$ reflects the conformation of a polymer chain or the density distribution of a particle and thus gives valuable information about the internal structure of microgels. Figure 2 shows ρ , calculated from the experimental values of R_g and R_h , as a function of temperature. The value of ρ at room temperature, 0.51, is significantly smaller than that predicted²⁵ for homogeneous hard spheres, namely 0.775. Typical ρ values for microgels in the range 0.3–0.6 have been reported.^{26,27} This means that particles become more tenuous in the outer region. It also implies heterogeneous swelling of the whole particle. This finding is consistent with polymerization kinetics, according to which the cross-linking density is higher inside the microgel particle than in the outer regions. In the swollen state, imperfections in cross-linking density lead to a decreasing density at the particle surface. The surface of the microgel is covered by dangling chains, which increase the hydrodynamic radius but have little influence on the radius of gyration.

At elevated temperatures, the mobility of the PVCL segments decreases and a more compact structure is formed. As a result, ρ increases and a value of 0.625 is reached at 50 °C. This value is, however, still lower than that of a homogeneous sphere. This deviation can be explained by the swollen surface of the microgel, which consists mainly of hydrophilic segments enriched with PVP.

SANS measurements were made at 15, 30, and 50 °C to investigate the structural changes of the microgel during the phase transition. To enlarge the range of the experimental results and improve the fitting quality, the static light scattering data were recalculated in SANS units by means of the following relation

$$I_{\text{SANS}} = \frac{R_\theta \Delta \rho^2 c_{\text{SANS}}}{K c_{\text{SLS}} N_A d_{\text{polym}}^2} \quad (1)$$

where d_{polym} is the polymer density, R_θ the Rayleigh ratio, N_A Avogadro's number, $\Delta \rho^2$ is the neutron scattering contrast factor, K is the contrast factor in SLS,

and c_{SLS} and c_{SANS} are the concentrations used for the measurements in SLS and SANS, respectively.

For the microgel in the swollen state (15 and 30 °C) the scattering intensity can be divided into two different terms. The first describes the large-scale features of the microgel (spherical particles). This region is followed by a steeply decreasing intensity at higher q . The second term describes the structure of the “bulk” gel inside. It is characterized by flattening of the scattering response at larger q as the polymer correlations inside the microgel are probed.

The form factor $P(q, r)$ for homogeneous monodisperse hard spheres of radius r is given by²⁸

$$P(q, r) = \left[\frac{3(\sin(qr) - qr \cos(qr))}{(qr)^3} \right]^2 \quad (2)$$

The combined DLS/SLS measurements suggest that the particle structure is inhomogeneous and fuzzy rather than uniform and with sharp boundaries. As mentioned above, the inhomogeneity is a result of cross-linking density gradient and the presence of the dangling chains. Thus, only lightly cross-linked or branched polymer chains are present on the surface. We use the structure factor for randomly branched polymers to describe the inhomogeneous particle surface.

$$P(q, s) = \frac{1}{1 + \frac{(qs)^2}{3}} \quad (3)$$

where the parameter s is the radius of gyration of randomly branched polymer chains. As this equation applies to randomly branched polycondensates²⁹ in free solution, however, its use can be only empirical here, owing to the different mechanism of branching and a fixed conformation of polymer chains on the surface.

Furthermore, in a real microgel system the size polydispersity of the particles must be taken into account. For this, the particle size distribution function $p(r)$ is assumed to be Gaussian.

$$p(r) = \frac{1}{\sqrt{2\pi}\sigma} \exp\left(-\frac{(r - R)^2}{2\sigma^2}\right) \quad (4)$$

where R is the average microgel particle radius and σ is the spread in the relative particle size. The resulting expression for the scattering intensity is thus

$$I_{\text{inh}}(q) = I_{\text{inh}}(0) \int_{R-3\sigma}^{R+3\sigma} \left[\frac{3(\sin(qr) - qr \cos(qr))}{(qr)^3} \right]^2 \times \frac{1}{\left(1 + \frac{(qs)^2}{3}\right)} p(r) dr \quad (5)$$

where $I_{\text{inh}}(0)$ is the limiting intensity at $q = 0$. Finally, the contribution from concentration fluctuations of the network in the core of the microgel may be approximated by an Ornstein–Zernicke expression^{30,31}

$$I_{\text{fluct}}(q) = \frac{I_{\text{fluct}}(0)}{1 + (q\xi)^2} \quad (6)$$

where $I_{\text{fluct}}(0)$ is the limiting intensity at $q = 0$ and ξ is the correlation length of the osmotic fluctuations in the

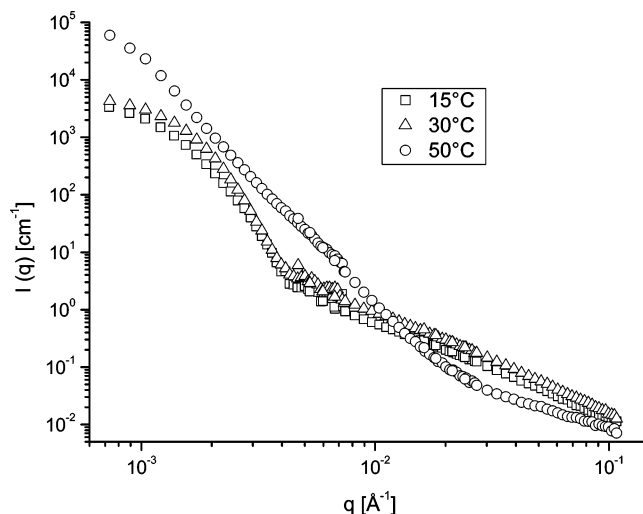


Figure 3. SANS intensity $I(q)$ at 15, 30, and 50 °C. Microgel concentration: 2.5 g/L.

swollen network. The complete expression for the scattering intensity from the swollen microgels thus becomes

$$I_{\text{microgel}}(q) = I_{\text{inh}}(0) \int_{R-3\sigma}^{R+3\sigma} \left[\frac{3(\sin(qr) - qr \cos(qr))}{(qr)^3} \right]^2 \times \frac{1}{1 + \frac{(qs)^2}{3}} p(r) dr + \frac{I_{\text{fluct}}(0)}{1 + (q\xi)^2} \quad (7)$$

Results of the fit of eq 7 to the 15 and 30 °C data are shown in Figure 4a,b.

Above the transition temperature, we have a phase-separated system in which the scattering arises from the interface between the collapsed polymer particle and the surrounding solvent. A strong deviation between the SLS and SANS measurements was observed at 50 °C at small q . This shows that the SANS response corresponds to surface scattering from large aggregates and that the particle structure factor for the spheres plays no role. The deviation from power-law behavior in the initial part of the SANS curve, where the product of the intensity and the sample thickness exceeds 10^4 , indicates multiple scattering. The aggregation probably results from the much higher microgel concentration used in SANS than in the light scattering measurements. It should be noted, however, that despite aggregation no macroscopic precipitation occurred, and the same scattering profile was observed for all measured concentrations.

For sharply defined smooth interfaces the structure factor is given by the Porod law³²

$$I_{\text{surf}}(q) = I_{\text{surf}}(0) q^{-4} \quad (8)$$

Surface roughness is the result of dangling chains, which are still in good solvent conditions at 50 °C (PVP-enriched chains). Correction of the intensity profile may be made in the same way as for the swollen state by introducing the scattering factor of randomly branched polymers. Besides, the scattering intensity at the larger q values can still be described by the Ornstein–Zernicke equation. To describe the results at 50 °C (see Figure

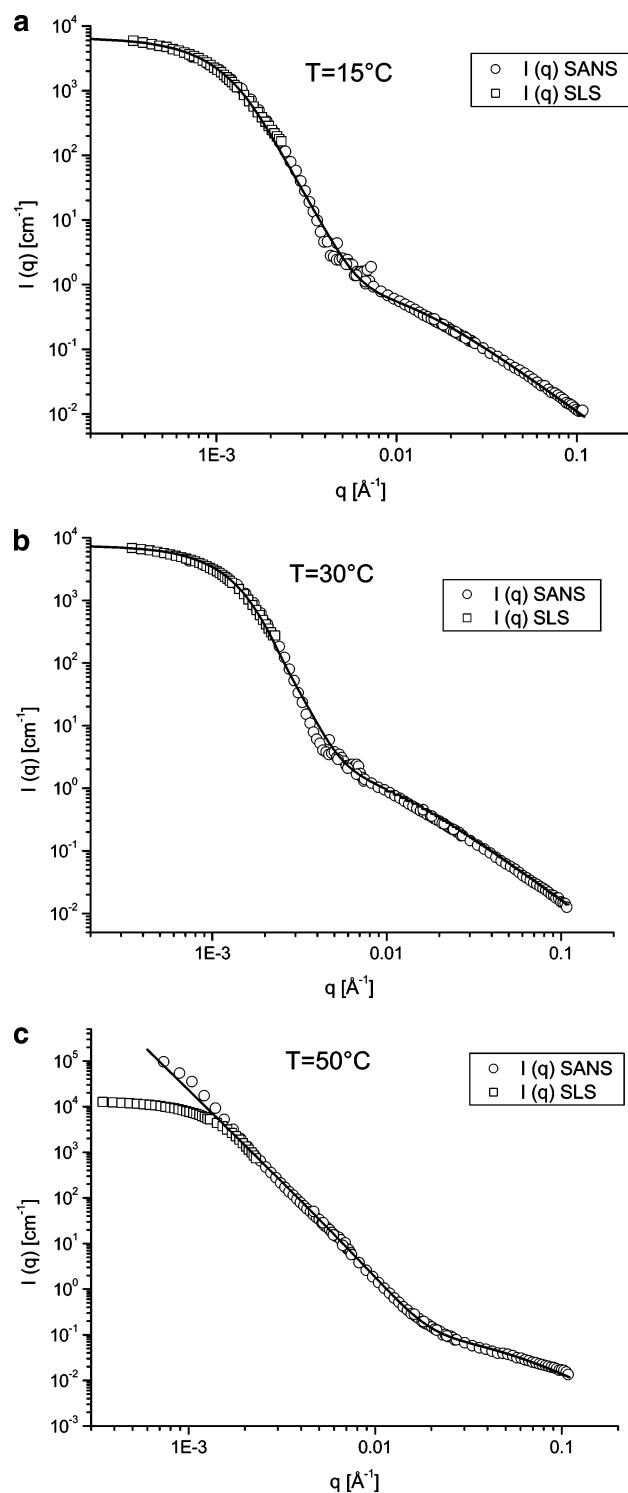


Figure 4. (a) Experimental data $I(q)$ (SLS and SANS) for 15 °C at microgel concentration 2.5 g/L and fit of eq 7 (solid line) to the 15 °C data. (b) Experimental data $I(q)$ (SLS and SANS) for 30 °C at microgel concentration 2.5 g/L and fit of eq 7 (solid line) to the 30 °C data. (c) Experimental data $I(q)$ (SLS and SANS) for 50 °C at microgel concentration 2.5 g/L and fit of eq 9 (solid line) to the 50 °C data.

4c), the following modified power law expression was therefore used.

$$I(q) = I_{\text{surf}}(0)q^4 \frac{1}{1 + \frac{(qs)^2}{3}} + \frac{I_{\text{fluct}}(0)}{1 + (q\xi)^2} \quad (9)$$

Results of the fits as well as results of SLS and DLS at the corresponding temperatures are summarized in Table 1. Surface roughness in the case of the 50 °C sample is found to be negligible. In the fits of Table 1 no correction was made for the resolution function of the instrument. The real values of σ are no doubt smaller than those quoted.

It can be seen that during heating from 15 to 30 °C the core of the microgel with radius R slightly decreases, and only a decrease of the branching length s of the lightly cross-linked chains in the shell can be observed. This fact is in a good agreement with the deswelling model proposed by Fernandez-Barbero et al.¹¹ for thermosensitive PNIPAm microgels. Further heating should lead to a decrease of the radius R , but it cannot be detected in our experiments. The polymer volume fraction of the collapsed microgel at 50 °C, calculated from the molecular weight, $M_w = 1.33 \times 10^9$ g/mol and the radius of gyration 1220 Å, is approximately 0.3. The characteristic size of the chains on the surface decreases to 10 Å or less on heating to 50 °C, indicating that surface roughness is negligible, while the correlation length in the core is 12 Å. This value of ξ is consistent with measurements on macroscopic polymer solutions at similar concentrations.³³ Some free hydrophilic chains, however, remain in good solvent condition, which is in agreement with the value of the ρ -parameter at this temperature. The presence of these chains would contribute to the colloidal stability of the individual particles and aggregates in SLS and SANS experiments, respectively.

Other models have been proposed to describe the structure of microgels (e.g., in which the shell is taken to have a Gaussian profile¹⁷). Although the numerical results differ slightly from the present findings, no significant qualitative difference is obtained. An estimate of the relative density of the polymer chains in the corona with respect to that in the core can be obtained in the following way. The radial distribution function $w(r)$ in the corona corresponding to the factor $1/[1 + (q^2s^2/3)]$ is proportional to

$$w(r) \propto \exp\left(-\sqrt{3} \frac{r}{s}\right) \quad (10)$$

The radius of gyration of the uniform core is $R_{\text{core}} = (3/5)^{1/2}R = 1550$ Å at 15 °C, while the measured total radius of gyration R_g is 1900 Å. If the density of the corona at $r = R$ were the same as that of the core, then the distribution (10) would yield for $R_g = 3150$ Å. For consistency of the measured value, the density of the corona at $r = R$ relative to the core must be approximately 0.2. It follows, by integration of eq 10, that the total mass of the corona is about 20% of that of the core. It is also notable that the effective total radius $R + s = 2950$ Å is significantly smaller than R_h . This means that the polymer chains in the corona extend at least twice as far as that indicated by the nominal thickness of the shell s .

The correlation length ξ found from analysis of the scattering curve is equal to 95 Å in the fully swollen state at 15 °C. This value is much larger than that measured in the case of the microgels^{8,11} or bulk gels¹ based on NIPAm (15–45 Å). However, it is comparable with the correlation length measured for a PNIPAm shell cross-linked on a polystyrene core.³⁴ The correlation length increases to 110 Å with heating to 30 °C as the transition temperature approaches and the intensity

Table 1. Results of the DLS and SLS (R_g , R_h , ρ) and Estimated Parameters (R , σ , s , ξ) of the Fits According to Eq 7 for 15 and 30 °C and Eq 9 for 50 °C

T [°C]	R_g [Å]	R_h [Å]	ρ	R [Å]	σ [Å]	s [Å]	ξ [Å]
15	1900	3720	0.51	2000	550	950	95
30	1620	2780	0.58	1800	400	600	110
50	1220	1940	0.63			<10	12

of the scattering from the core increases. In the bulk gel, the correlation length and the intensity diverge at this temperature.¹ Similar behavior has been observed in PNIPAm microgels,¹¹ where the correlation length in the core was found to increase in the vicinity of the transition temperature. Above the transition temperature the microgel collapses and the correlation length decreases to 12 Å at 50 °C. This decrease of ξ is to be expected since at higher temperatures the microgel network is denser.

4. Conclusions

Thermosensitive microgels based on *N*-vinylcaprolactam and *N*-vinylpyrrolidone were prepared by precipitation copolymerization. The presence of hydrophilic comonomer during cross-linking leads to formation of a stable dispersion of large particles.

SLS, DLS, and SANS measurements of the structure of the microgels show a strong decrease in the radius of gyration R_g and the hydrodynamic radius R_h during the phase transition near 30 °C. In agreement with other studies on similar systems, the microgel consists of dense core surrounded by a diffuse corona, the mass of which is about one-fifth of that of the core. Below the transition temperature, the apparent thickness of the corona required to produce an acceptable fit to the SANS results is too small to account for the value found for R_h . This finding implies that the polymer chains are more extended than either the radius of gyration s of branched polymers or a random coil. A small number of polymer chains must therefore extend much further than the average shell thickness. At 50 °C Porod scattering is observed as the corona collapses on the surface of the core. In this state the characteristic ratio ρ is only slightly smaller than the value for a uniform sphere, 0.775. The smooth surface of the microgel must therefore be sparsely decorated with excrescences of hydrophilic polymer segments.

Acknowledgment. The authors are grateful to the Institut Laue Langevin (ILL) for access to the D11 instrument. We also thank Mrs. Ch. Meissner (TU Dresden) for static light scattering measurements. S. Richter acknowledges financial support from the Deutsche Forschungsgemeinschaft (DFG) (Grant RI 1079/1-2).

References and Notes

- (1) Shibayama, M.; Tanaka, T. *J. Chem. Phys.* **1992**, *97*, 6829.
- (2) Horkay, F.; Burchard, W.; Hecht, A.-M.; Geissler, E. *Macromolecules* **1993**, *26*, 3375.
- (3) Moussaid, A.; Candau, S. J.; Joosten, J. G. H. *Macromolecules* **1994**, *27*, 2102.
- (4) Shibayama, M. *Macromol. Chem. Phys.* **1998**, *199*, 1 and references cited therein.
- (5) Ngai, T.; Wu, C.; Chen, Y. *J. Phys. Chem. B* **2004**, *108*, 5532.
- (6) Wu, X.; Pelton, R. H.; Hamielec, A. E.; Woods, D. R.; McPhee, W. *Colloid Polym. Sci.* **1994**, *272*, 476.
- (7) Kratz, K.; Hellweg, T.; Eimer, W. *Polymer* **2001**, *42*, 6631.
- (8) Kratz, K.; Lapp, A.; Eimer, W.; Hellweg, T. *Colloids Surf. A* **2002**, *197*, 55.
- (9) Saunders, B. R.; Crowther, H. M.; Morris, G. E.; Mears, S. J.; Cosgrove, T.; Vincent, B. *Colloids Surf. A* **1999**, *149*, 57.
- (10) Saunders, B. R. *Langmuir* **2004**, *20*, 3925.
- (11) Fernandez-Barbero, A.; Fernandez-Nieves, A.; Grillo, I.; Lopez-Cabarcos, E. *Phys. Rev. E* **2002**, *66*, 051803.
- (12) Burchard, W.; Kajiwara, K.; Nerger, D. *J. Polym. Sci., Polym. Phys. Ed.* **1982**, *20*, 157.
- (13) Kunz, D.; Burchard, W. *Colloid Polym. Sci.* **1986**, *264*, 498.
- (14) Varga, I.; Gilanyi, T.; Meszaros, R.; Filipcsei, G.; Zrinyi, M. *J. Phys. Chem. B* **2001**, *105*, 9071.
- (15) Svaneborg, C.; Pedersen, J. S. *Phys. Rev. E* **2001**, *64*, 010802.
- (16) Pedersen, J. S.; Svaneborg, C. *Curr. Opin. Colloid Interface Sci.* **2002**, *7*, 158.
- (17) Stieger, M.; Richtering, W.; Pedersen, J. S.; Lindner, P. *J. Chem. Phys.* **2004**, *120*, 6197.
- (18) Meyer, S.; Richtering, W. *Macromolecules* **2005**, *38*, 1517.
- (19) Tager, A. A.; Safronov, A. P.; Berezyuk, E. A.; Galaev, I. Y. *Colloid Polym. Sci.* **1994**, *272*, 1234.
- (20) Vihola, H.; Laukkanen, A.; Hirvonen, J.; Tenhu, H. *Eur. J. Pharm. Sci.* **2002**, *16*, 69.
- (21) Laukkanen, A.; Wiedmer, S. K.; Varjo, S.; Riekkola, M.-L.; Tenhu, H. *Colloid Polym. Sci.* **2002**, *280*, 65.
- (22) Peng, S.; Wu, C. *Macromolecules* **2001**, *34*, 568.
- (23) Boyko, V.; Richter, S.; Pich, A.; Arndt, K.-F. *Colloid Polym. Sci.* **2003**, *282*, 127.
- (24) McPhee, W.; Tam, K. C.; Pelton, R. H. *J. Colloid Interface Sci.* **1993**, *156*, 24.
- (25) Kunz, D.; Thurn, A.; Burchard, W. *Colloid Polym. Sci.* **1983**, *261*, 635.
- (26) Burchard, W. *Adv. Polym. Sci.* **1983**, *48*, 1.
- (27) Schmidt, M.; Nerger, D.; Burchard, W. *Polymer* **1979**, *20*, 582.
- (28) Rayleigh, J. W. *Proc. R. Soc. London* **1914**, *A90*, 219.
- (29) Burchard, W. *Macromolecules* **1977**, *10*, 919.
- (30) Bueche, F. *J. Colloid Interface Sci.* **1970**, *33*, 61.
- (31) Soni, V. K.; Stein, R. S. *Macromolecules* **1990**, *23*, 5257.
- (32) Porod, G. *Kolloid Z.* **1951**, *2*, 83.
- (33) Horkay, F.; Hecht, A.-M.; Stanley, H. B.; Geissler, E. *Eur. Polym. J.* **1994**, *30*, 215.
- (34) Seelenmeyer, S.; Deike, I.; Rosenfeld, S.; Norhausen, Ch.; Digenouts, N.; Ballauff, M.; Narayanan, T.; Lindner, P. *J. Chem. Phys.* **2001**, *114*, 10471.

MA050548W